Long ferromagnetic correlation length in amorphous $TbFe_2$

F. Hellman and A. L. Shapiro
Department of Physics, University of California, San Diego, La Jolla, California 92093

E. N. Abarra
Toyota Technological Institute, Nagoya, Japan

R. A. Robinson, R. P. Hjelm, and P. A. Seeger
Manuel Lujan Jr. Neutron Scattering Center, Los Alamos National Laboratory, Los Alamos, New Mexico 87545

J. J. Rhyne
Department of Physics, University of Missouri, Columbia, Missouri 65211

J. I. Suzuki
Japan Atomic Energy Research Institute, Tokai-Mura, Ibaraki-Ken 319-11, Japan
(Received 29 October 1998)

Small-angle neutron scattering (SANS) and magnetic-force microscopy (MFM) have been used to characterize the temperature dependence of the ferromagnetic correlation length and the domain structure in amorphous $TbFe_2$ below its magnetic ordering temperature. Amorphous $TbFe_2$ is classified as a random anisotropy magnet, in the exchange-dominated limit, and previous SANS observations had shown a correlation length limited to 50 Å at low temperatures. In the present study, samples were prepared by both sputtering and electron beam coevaporation and were either grown or preannealed at 200 °C in order to permit measurements above T_c without structural relaxation. Samples grown by vapor deposition processes possess a large macroscopic perpendicular anisotropy constant K_u, which can be reduced or eliminated by annealing. A strong SANS signal is seen in all samples, with a magnitude strongly correlated with the temperature-dependent sample magnetization and with the inverse length scale of the domain structure seen in MFM. For all samples, the magnetic correlation length determined from SANS is 300–500 Å in the thermally demagnetized state, and increases beyond measurement range after magnetizing. This long correlation length is consistent with theoretical predictions of a ferromagnetic ground state in exchange-dominated random anisotropy magnets in the presence of coherent anisotropy. The SANS signal is dominated by a Lorentzian squared term, which is best understood as resulting from ferromagnetic domains with meandering domain walls, similar to the Debye-Bueche model developed for materials consisting of two strongly segregated, interpenetrating phases. [S0163-1829(99)01317-X]

I. BACKGROUND

The structural and magnetic properties of amorphous rare-earth–transition-metal (a-R-TM) alloys and particularly amorphous $TbFe_2$ have been studied extensively over the last 20 years. For most thin films, the growth-deposition process induces a perpendicular uniaxial magnetic anisotropy K_u.[1–5] K_u together with a suitable T_c, coercivity, Kerr rotation, and optical reflectivity, have made quaternary alloys related to a-$TbFe_2$ the materials of choice for magneto-optic recording.[6,7] The strength and (approximately) random orientation of the local magnetic anisotropy of the Tb ion, tends to pull the local magnetic moment away from a collinear arrangement. Consequently, studies of amorphous $TbFe_2$ were prominent in the development of random magnetic anisotropy (RMA) theory, a branch of the field of random magnetism.[8–20]

The exchange interaction between Fe ions is primarily ferromagnetic (due to a relatively large Fe-Fe separation) while the interaction between R and Fe ions is antiferromagnetic, giving rise to a ferrimagnet (more properly termed a sperimagnet due to the random anisotropy of the Tb).[21] Comparisons to a-Y-Fe (Refs. 9 and 22) suggest that there is still significant exchange frustration from some antiferromagnetic Fe-Fe interactions, but these are somewhat offset by the R-Fe interactions which are not frustrated, making this a reasonably good system for studying random anisotropy effects. Harris, Plischke, and Zuckermann[12] introduced the following Hamiltonian for RMA materials with predominantly ferromagnetic exchange:

$$H = -\frac{1}{2} J_{\mathrm{ex}} \sum_{ij} \mathbf{S}_i \cdot \mathbf{S}_j - \frac{1}{2} D \sum_i (\hat{\mathbf{n}}_i \cdot \mathbf{S}_i)^2 - \mathbf{H} \cdot \sum_i \mathbf{S}_i . \quad (1)$$

The first term is a Heisenberg exchange with average strength J_{ex}, the second is the random anisotropy term, and the third is the interaction with an external field **H**. The anisotropy term approximates the low symmetry of the amorphous structure with a uniaxial anisotropy of (average) strength D and direction $\hat{\mathbf{n}}_i$ which varies from site to site. There have been a number of theoretical and experimental

reviews of this problem.[11,13–15] For $D/J_{ex} \gg 1$, theory and simulation show an exponentially damped spin-spin spatial correlation function, with a finite ferromagnetic correlation length R_f which is short but considerably larger than the lattice constant a, and zero net magnetization in zero field.[18,23,24] This state has been termed speromagnetic or correlated spin glass and has zero macroscopic moment. Recent theoretical work has suggested that this state is strictly speaking paramagnetic even at $T=0$, with all time-averaged local moments $\langle S_i \rangle = 0$.[25] However, this paramagnetic state is glassy, and it seems likely that for all experimentally realizable times, high D/J_{ex} material will appear speromagnetic, with nonzero local $\langle S_i \rangle$.

The weak anisotropy limit $D/J_{ex} < 1$ is theoretically more complex. As an approximation to a low D/J_{ex} material, R. Fisch recently performed a computer simulation for a two-component RMA material, one with $D/J_{ex} = \infty$ and concentration x and the other component with $D/J_{ex} = 0$ and concentration $1-x$. This simulation shows a crossover from the above-described glassy paramagnet behavior at high x to a quasi-long-range ordered (QLRO) state for $x < 0.6$, suggesting that low D/J_{ex} materials might exhibit this QLRO state.[25] The QLRO state has no true long-range magnetic order, but has power-law spin-spin correlations (instead of exponentially damped as in the speromagnetic state) and a susceptibility and magnetic correlation length which diverge at the phase transition from the paramagnetic state. Fisch also found a QLRO state for spins confined to a plane (number of spin components $m=2$), in three dimensions ($d=3$) even for $D/J_{ex} \gg 1$,[26] and in the related random-field problem in $d=3$.[27]

Because of the strength of the exchange coupling, it is nearly certain that a-$TbFe_2$ is in this weak anisotropy, exchange-dominated limit with $D/J_{ex} \sim 0.3-0.7$.[28] Recent specific-heat measurements of a-$TbFe_2$ found a sharp thermodynamic peak at the same temperature T_c as that measured magnetically, with an apparent critical exponent consistent with the calculations of Fisch.[25,29] Small-angle neutron scattering studies[8] on a-$Tb_{32}Fe_{68}$ (extremely rapidly sputtered, with no macroscopic anisotropy K_u) showed a noncollinear magnetic structure and a finite ferromagnetic correlation length below the transition temperature T_c. Specifically, analysis of the SANS data on this and other amorphous rare-earth alloys[30] were consistent with a scattering cross section of the form:

$$I(Q) = \frac{A}{Q^2+\kappa^2} + \frac{B}{(Q^2+\kappa^2)^2}, \tag{2}$$

where the first (Lorentzian) term predominantly represents fluctuations in the spin system (e.g., spin waves) and the second (Lorentzian-squared) term arises from scattering from static regions of spin ordering. This form of scattering was proposed as that for the RMA-induced speromagnetic state, but would also be observed whenever there is a static wandering of magnetization with an exponential decay of the correlation function $\langle \sigma(\mathbf{r}_1)\sigma(\mathbf{r}_2)\rangle \propto \exp(-\kappa|\mathbf{r}_1-\mathbf{r}_2|)$, such as would be found for magnetic domains separated by meandering domain walls. This latter effect is analogous to strongly segregated, randomly interpenetrating phases in the Debye-Bueche model.[31] The quantity κ that appears in both terms of Eq. (2) is the inverse of the spin-correlation length ($\kappa = R_f^{-1}$) where R_f describes the range of essentially uniform order. The correlation length found in the work on rapidly sputtered a-$Tb_{32}Fe_{68}$ increased from ~10 Å at 450 K to ~135 Å below $T_c = 409$ K, and then decreased to ~50 Å at low temperature.[8] The coefficient B of the Lorentzian-squared term can be related to the magnetization within a cluster or domain, $B \alpha |M|^2 \kappa$, in either model (randomly interpenetrating domains or speromagnet). This proportionality was confirmed in Ref. 8. In the Debye-Bueche model, $B = 8\pi\kappa(\Delta\rho)^2\Phi(1-\Phi)$, where $\Delta\rho$ is the change in scattering length density between the two phases, Φ is the fraction of phase 1, and $(1-\Phi)$ is the fraction of phase 2. The magnetic scattering length for a single magnetic moment equals $0.27 \times 10^{-12}\mu$ (in cm) where μ is the number of Bohr magnetons. Therefore, the magnetic scattering length density $\rho = 0.27 \times 10^{-12} M/\mu_B$ where M is the magnetization density (emu/cc) and μ_B is the Bohr magneton. For magnetic domains in a material with uniaxial anisotropy, $\Delta\rho = 2\rho$ and therefore is proportional to $2M$, and Φ and $1-\Phi$ would normally both be equal to 0.5 in the demagnetized state. B is therefore expected to be given by $8\pi\kappa(0.27 \times 10^{-12} M/\mu_B)^2$.

A different form for analyzing SANS data has been suggested for the QLRO state. Specifically, for the QLRO state,

$$I(Q) = \frac{A}{Q^2} + \frac{B}{(Q^2)^x} \tag{3}$$

with $x = 1.5$ for $m=3$, $d=3$,[25] and $x=1.2$ for $m=2$, $d=3$.[26] The correlation length is in theory infinite, leading to the form shown above, but in practice will be limited by instrument resolution or sample imperfections, introducing κ into the expression above. The data of Rhyne *et al.* in Ref. 8 was reanalyzed (in the $m=2$, $d=3$ limit) and was shown to fit the expected form for this QLRO state.[26]

When considering RMA materials, it is necessary to consider the possibility of correlations in the set of local anisotropy axis directions $\hat{n}_i$. There can be correlations in the directions of neighboring $\hat{n}_i$, introducing what is called an orientational correlation length R_a.[20] It has been suggested that in the amorphous state, the orientational correlation length could/should be much longer than the positional correlation length, which tends to be only of the order of an interatomic distance a.[32] R_a has never been determined by direct structural methods but magnetization studies of a-RFeB suggested $R_a \sim 100$ Å, far greater than the ~10 Å atomic/structural correlation length.[33] R_a causes the exchange energy J_{ex} to be replaced by an effective exchange energy which is reduced by $(a/R_a)^2$. Therefore, R_a impacts the effective ratio of anisotropy to exchange energy and hence the ferromagnetic correlation length[20,33,34]. Following Chudnovsky's work, the ferromagnetic correlation length is

$$R_f = \left(\frac{A}{K_r}\right)^2 \frac{1}{R_a^3}, \tag{4}$$

where K_r is the macroscopic variable characterizing the random anisotropy and is proportional to D.[28] R_f decreases with increasing R_a, but can never be less than R_a.

The second type of correlation in $\hat{n}_i$ is a preference for a given spatial direction, e.g., along the growth direction of a thin film, leading to macroscopic magnetic anisotropy with magnitude K_u. It has been theoretically demonstrated that the ferromagnetic (FM) state can be recovered as the ground state in the presence of sufficiently large but finite K_u.[19,20,25] In this FM state, the random anisotropy still produces a wandering of the magnetization and hence leads to SANS signals of the form seen in Eq. (2). It is clear from a variety of magnetic measurements, including the ability to use this material for magneto-optic recording, that high K_u a-$TbFe_2$ is capable of sustaining perpendicular domains, even in a zero-field-cooled state so that magnetic history is not simply trapping the system in a nonequilibrium state. To consider the magnitude of K_u necessary to induce a crossover, we follow Chudnovsky's work and introduce the ratio $H_u/H_s = K_u A^3/K_r^4 R_a^6 = K_u R_f^2/A$ where $H_s = 2(K_r^4/A^3 M)R_a^6$ is a characteristic crossover field for the material and $H_u = 2K_u/M$ is the coherent anisotropy field.[20] When $H_u/H_s < 1$, the properties of the RMA magnet are not significantly altered by K_u; for example, in the speromagnetic state, R_f is still given by Eq. (4) above. However, when $H_u/H_s > 1$, the system is converted to what is called a ''ferromagnet with wandering axis.'' Here, the magnetization lies more or less along one of the two coherent anisotropy easy-axis directions, as in a conventional uniaxial ferromagnet, but within a domain, the magnetization wanders in direction with a characteristic tilt angle (away from the coherent anisotropy direction) $\sim (H_u/H_s)^{1/4}$ α $(a/R_a)^{3/2}$ and a perpendicular correlation length which can be written as $R_f^{\perp} = (A/K_u)^{1/2}$ (like R_f, $R_f^{\perp}$ can never be less than an in-plane orientational correlation length $R_a^{\perp}$).

Previous work on a-$TbFe_2$ thin films has shown that the coherent anisotropy K_u increases with increasing substrate temperature T_s during deposition, from less than 1×10^6 erg/cm^3 to greater than 1×10^7 erg/cm^3.[2,35] Annealing at temperatures near 620 K can reduce or eliminate this anisotropy, without inducing observable crystallization.[5,35,36] The magnitude of K_u can thus be varied over two orders of magnitude by choice of deposition conditions and/or annealing. Estimates of the necessary value of K_u needed to restore LRO are $\sim 4 \times 10^6$ ergs/cm^3 at low temperature and several times lower at room temperature.[37] The properties of an initially high K_u sample should, therefore, depend strongly on annealing which reduces and then eliminates K_u (in which state the sample should be describable as an $m=3$, $d=3$ RMA material). With further annealing, tensile strains plus magnetostriction together with dipolar (shape) anisotropy make K_u significantly negative ($K_u < 0$ means a planar anisotropy, which should be describable as an $m=2$, $d=3$ RMA state). The present study was undertaken to investigate the form of the small-angle scattering and the ferromagnetic correlation length in the presence and absence of perpendicular anisotropy K_u.

II. SAMPLE PREPARATION AND CHARACTERIZATION

Samples were grown from separate Tb and Fe sources using two methods: (1) *e*-beam coevaporation in a UHV chamber and (2) magnetron cosputtering with an LN_2-cooled shroud providing a high vacuum environment. Overlayers of 300 Å Nb or Cu were used to prevent oxidation. The pressure before evaporation is $< 3 \times 10^{-9}$ Torr and $< 1 \times 10^{-8}$ Torr during growth; pressures during sputtering inside the LN_2 shroud are similarly low. Samples were grown on substrates held at different temperatures T_s in order to obtain different values for the perpendicular anisotropy K_u. Typical deposition rates were 0.5–5 Å/s. There has been extensive x-ray scattering, TEM, neutron scattering, and extended x-ray absorption fine structure studies on sputtered R-T alloys in the past showing the amorphous nature of the samples and the absence of nanocrystallites.[1–3,5,8,38] X-ray, TEM, Rutherford backscattering, and Auger profiling studies have been performed on both our *e*-beam evaporated and sputtered samples.[36,39] X-ray measurements were specifically made on the thick (1–1.5 μm) samples prepared for this study. TEM images for a-$Tb_{28}Fe_{72}$ grown at room temperature show diffuse SAD rings. For these thin TEM samples (300 Å thickness), the bright-field image shows evidence of density fluctuations with a length scale of 100–300 Å, presumably related to a columnar microstructure. Such microstructure is common in evaporated amorphous materials and is not evident in the sputtered films, nor in the evaporated films grown at 523 K.[40] For *e*-beam evaporated a-$Tb_{28}Fe_{72}$ grown at 523 K, the bright-field image is featureless and the selected area diffraction (SAD) rings are diffuse. Films grown at room temperature and annealed at 523 K appear identical in TEM to the as-deposited films, including the density fluctuations; in particular no crystallization was detected, consistent with earlier work on annealed a-Tb-Fe.[2,5] Auger depth profiling showed no O (to the resolution of the measurement $\sim$1%) in a-$Tb_{28}Fe_{72}$ and uniform Tb/Fe composition for both sputtered and evaporated samples.

Small-angle neutron scattering (SANS) measurements were performed using the low-Q diffractometer (LQD) at the Los Alamos Neutron Science Center[41] (LANSCE) and the SANS-J machine at the JRR-3M reactor at the Japan Atomic Energy Research Institute (JAERI). Both instruments employ large two-dimensional multiwire position-sensitive area detectors to measure scattering intensity I as a function of position on the detector. Data from SANS-J is mapped directly into intensity (after averaging over the appropriate range of azimuthal angles) as a function of momentum transfer, $Q = 4\pi/\lambda \sin\theta$, where λ is the incident neutron wavelength and 2θ is the scattering angle. LQD uses time-of-flight techniques; the data from this instrument are reduced using standard techniques[42,43] to give the intensity I in absolute units of differential cross section per unit area $dP/d\Omega$ (cm^2/cm^2) as a function of magnitude and direction of scattering vector $\mathbf{Q}$. Dividing the intensity by the sample thickness in cm gives the differential cross section per unit volume, usually noted as $d\Sigma/d\Omega$ (cm^{-1}). We achieved consistent results on LQD and SANS-J, even though the former is a broadband time-of-flight SANS machine at a spallation source, while the latter is a constant-wavelength machine at a reactor. At JAERI, the wavelength used was 6.1 Å for one set of data and 10 Å for another, with a resolution $\Delta\lambda/\lambda$ of 13%. At LQD, wavelengths between 4.118 and 15.151 Å with a resolution $\Delta\lambda/\lambda$ of 10% were used for the analysis. Shorter wavelengths were not used in the analysis due to interference from multiple

Bragg reflections from the Si substrate.

Our samples were mounted with the film surface perpendicular to the incident neutron beam. This geometry ensures that **Q** is always approximately in the plane of the film. The magnetic scattering is sensitive only to spin components perpendicular to **Q**. The SANS signal $I(\mathbf{Q})$ is proportional to the Fourier transform of the magnetization density $M(\mathbf{r})$ in the sample. In the range of Q accessible to experiment the scattering arises from correlated magnetic regions that are of finite size. In particular, the uniform magnetization of a single-domain ferromagnet is not measured, since this scattering would occur only at $Q=0$, a value not measurable in SANS. Measurements were made either in a turbo-pumped vacuum furnace or in a He cryocooler to permit sample temperatures from 20 to 473 K. Background, transmission, and calibration standards were measured to permit absolute measurements of scattering.[42] Absorption by the sample was measured and found to be negligible.

Magnetic-force microscope (MFM) images were made using several types of commercial magnetic tips. Low coercivity, and low and high moment tips gave similar results, although due to the large $M_r t$ product, the best results were obtained using low moment tips. Here M_r is the remanent moment and t is the magnetic film thickness. The scan height was ~40 nm (plus the thickness of the Nb overlayer); features observed were much larger laterally than this height. The MFM is primarily sensitive to magnetic charges, thus to domain walls, but especially for perpendicularly magnetized samples, domain structure can also be inferred. Atomic-force microscopy (AFM) using the MFM tip in a tapping mode was used to measure surface height features; root-mean-square roughness in all cases was 10 Å or less.

In both SANS and MFM studies the samples were 1 to 1.5 microns thick on (100) Si substrates (Si native oxide was not removed). To obtain adequate SANS intensity several samples were stacked together.

III. SANS AND MFM RESULTS

A. Evaporated perpendicular anisotropy sample

Figure 1 shows the intensity of scattering $I=dP/d\Omega$ at 300 K as a function of scattering vector **Q** in the x-y detector plane for an evaporated sample with large perpendicular anisotropy K_u. This sample was grown at 473 K. T_c of this sample determined from the kink method of magnetization versus temperature is 448 K. Figure 1(a) shows data taken with the sample in the thermally demagnetized state (either an as-prepared sample or one which has been cycled to above T_c and then brought back to 300 K in zero field; these two states were shown experimentally to be the same for this sample which was grown at high temperature). There is a strong in-plane asymmetry; the magnitude of scattering in the x and y directions differ by an order of magnitude at any given Q. Figure 1(b) shows data on the identical sample after magnetizing (in a perpendicular field of 10 kOe) at room temperature and then removing the applied field. The scattering in this remanent state is nearly isotropic in plane and is well over an order of magnitude smaller than seen in Fig. 1(a). Magnetic hysteresis loops show the magnetization to be close to zero in both cases (this thick sample with large M_s has low coercivity and hence demagnetizes nearly completely in zero field). Magnetization measurements show very little asymmetry in the x and y direction properties of the sample; torque curves measured with the magnetic field applied in the x-z plane are identical to those measured with field applied in the y-z plane, while hysteresis curves measured for the x direction differ slightly from those for the y direction (the easy axis is strongly along z). The in-plane SANS asymmetry seen in the demagnetized state is completely correlated with the direction of incident atomic beams during growth of the films; we have prepared films with the sample plate rotated azimuthally by 30 degrees with respect to the incident beam directions and have found that the SANS-observed asymmetry rotates as well.

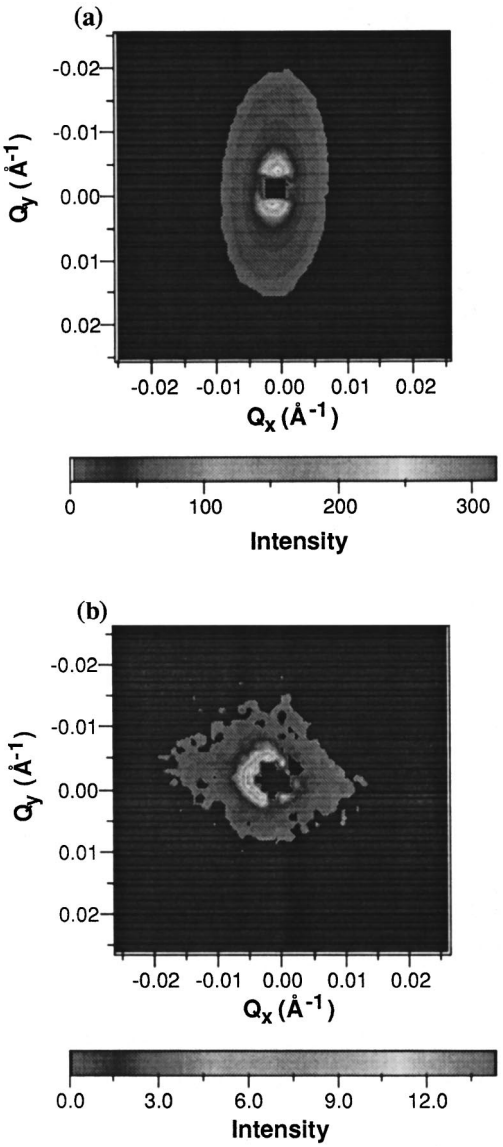

FIG. 1. SANS intensity $I(\mathbf{Q})$ shown as a gray scale for evaporated perpendicular K_u a-$TbFe_2$ (grown at 473 K) measured at 300 K. Neutrons are incident along the z axis (perpendicular to film plane) and the scattering vector is in-plane. Total sample thickness is 10.5 μm (seven samples each 1.5 μm). (a) Samples in the thermally demagnetized state. (b) Samples in the remanent state after applying saturating magnetic field (10 kOe applied perpendicular) at 300 K. Magnetic hysteresis loops show low remanence ($<20\%$ M_s). $K_u=1.0\times10^7$ ergs/cc and $M_s=340$ emu/cc at 300 K.

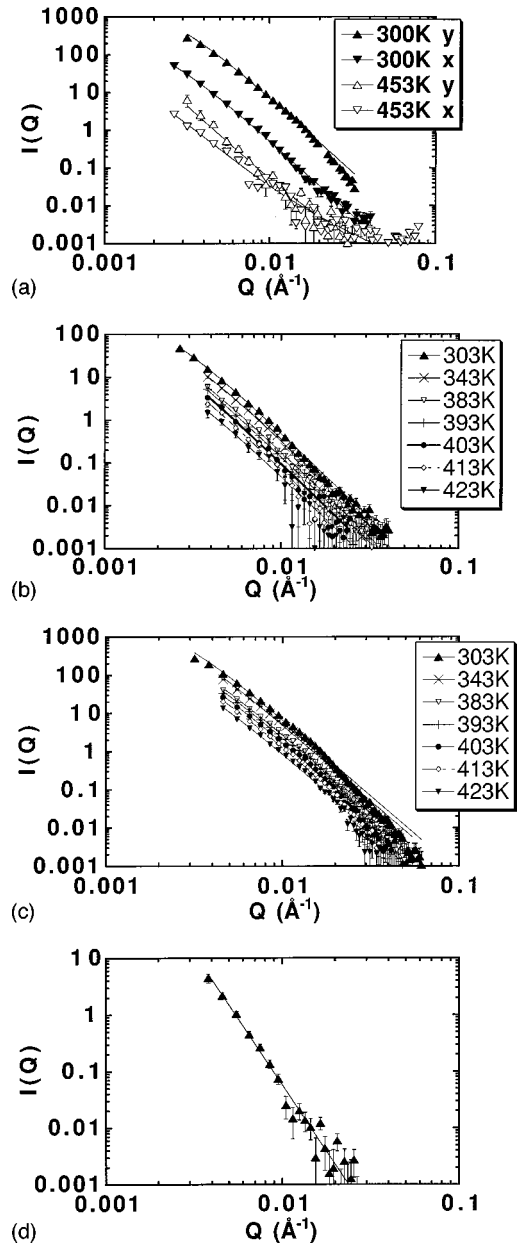

FIG. 2. (a) $I(\mathbf{Q})$ for evaporated perpendicular K_u a-$TbFe_2$ measured at 300 K and at 453 K for data averaged over 30 degree segments along x or y. (b) and (c) Temperature dependence of the magnetic contribution to $I(Q)$ x and y directions. (d) Magnetic contribution to $I(Q)$ at 300 K for the same sample in the remanent state (10 kOe applied perpendicular to film then removed). Data are in absolute units of differential scattering cross section per unit area $dP/d\Omega$ (cm^2/cm^2) (1 barn$=10^{-12}$ cm^2). Sample total thickness 10.5 μm (seven samples each 1.5 μm) for (a)–(c); (d) six samples for a total of 9 μm. The 458 K ($>T_c$) $I(Q)$ has been subtracted from (b), (c), and (d). Fits shown in (b) and (c) are Lorentzian squared (Lorentzian term was negligible) with a correlation length of 500 Å for the y direction and 600–700 Å for the x direction at all temperatures. In the remanent state of (d), the best fit was $1/Q^x$ with $x=4.7$.

Measurements made at higher temperatures on the same sample show steady decrease in SANS scattering intensity $I(Q)$ with increasing temperature. Data are shown in Figs. 2(a)–2(c) for the thermally demagnetized state as a function of temperature. Data were averaged over 30 degree segments along either the x or y in-plane directions. Figure 2(a) shows $I(Q)$ at room temperature and at 453 K (180 °C) for both directions. By 453 K, above the magnetic ordering temperature of the sample, $I(Q)$ has decreased by over an order of magnitude and the in-plane asymmetry is greatly reduced. Figures 2(b) and 2(c) show $I(Q)$ for the x and y directions, respectively, as a function of temperature. Figure 2(d) shows $I(Q)$ for the same sample in the magnetic remanent state at 300 K. The 458 K ($>T_c$) intensity that is largely nonmagnetic, structural scattering has been subtracted from Figs. 2(b)–2(d).

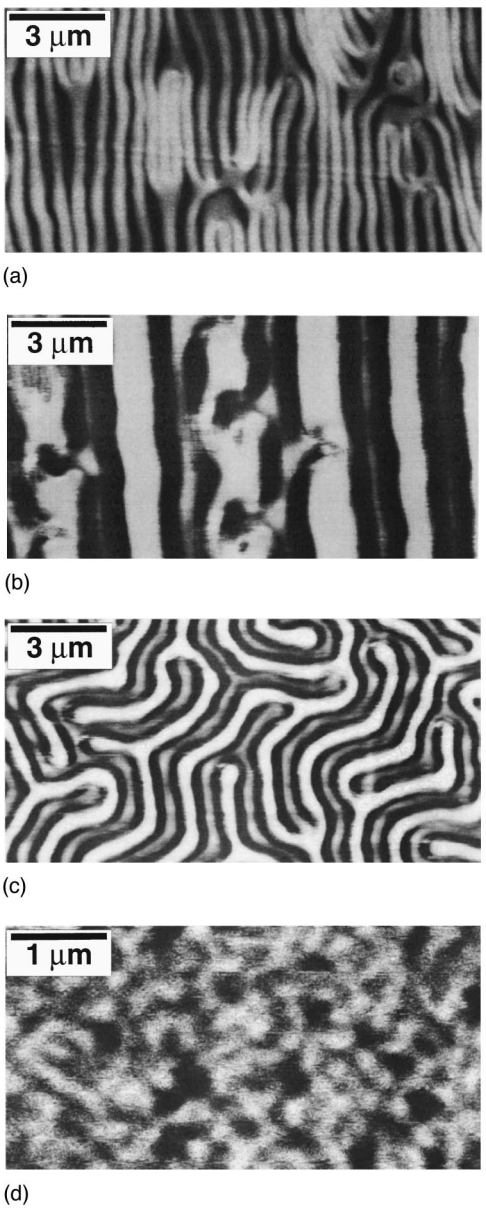

FIG. 3. MFM data for a piece of the same perpendicular K_u sample whose SANS results were shown in Figs. 1 and 2. (a) thermally demagnetized state, (b) remanent state after applying 10 kOe field perpendicular to sample and then turning off field, and (c) after an ac demagnetization (sample was rotated while applying a slowly decaying magnetic field). (d) thinner (2000 Å thickness) but otherwise identical perpendicular K_u sample in thermally demagnetized state.

Figure 3 shows magnetic-force microscopy measurements

taken at 300 K on a piece of the same sample used for SANS measurements, in the thermally demagnetized (a) and remanent (b) states. For MFM images of the thermally demagnetized state, the samples were first annealed at 453 K in vacuum ($P<5\times10-7$ Torr) for half an hour before imaging at room temperature. For the remanence images, the samples were saturated along a magnetic easy-axis direction (perpendicular for this sample) in fields of 15 kOe and were taken out of the magnet after the applied field was turned off. Although magnetic hysteresis loops showed the net magnetization to be nearly identical for both states ($M_r<0.2M_s$), the domain structure is very different. In the thermally demagnetized state, the domains are narrow (3000 Å) along the in-plane direction parallel to the incident atomic beams and extremely elongated parallel to the other in-plane direction. In the remanent state, the domains are approximately an order of magnitude wider. These differences are presumably related to details of domain-wall nucleation and motion. Figure 3(c) shows the same sample after an ac demagnetization; specifically, the sample was rotated in a decaying applied magnetic field. Here the domains show no sign of asymmetry, suggesting that the asymmetric domain-wall pinning or nucleation is a relatively weak effect. Figure 3(d) shows an MFM image for a thinner sample (2000 Å thickness) prepared identically to the samples shown in Figs. 3(a)–3(c); K_u and M_s are the same. In this thinner sample, the domains show no asymmetry in the demagnetized state. We suggest that the asymmetry observed in the thicker sample is a result of a large scale structure which develops as the film grows.[44] This large scale structure does not manifest itself in any significant difference in magnetic properties other than the domain size asymmetry seen in Figs. 3(a) and 3(b), nor in any observable structure in AFM images of the sample. We note however that the AFM images were taken with a 200 Å Nb overlayer covering the a-$TbFe_2$.

B. Evaporated in-plane anisotropy sample

Figure 4(a) shows SANS $I(Q)$ data on a sample with in-plane magnetic anisotropy. Data taken at 473 K (above T_c) were subtracted from the lower temperature data in order to eliminate the structural contribution to the SANS signal. This sample was grown at room temperature and then annealed at 573–623 K for 2 h to eliminate K_u and to make the sample resistant to further relaxation on measuring to 473 K. Before annealing, this sample had moderately large perpendicular K_u. After annealing, the anisotropy is strongly in-plane (negative K_u) due to large tensile strains plus shape anisotropy. $M(H)$ loops taken at room temperature show that the sample has a strong in-plane easy axis, along the x direction (approximately parallel to the incident atomic beams during growth). Despite the asymmetry in the $M(H)$ loops, the SANS data are isotropic in plane, so a full angular average is used for determining $I(Q)$. As the magnetization is in-plane, the contrast seen in the MFM images [Fig. 4(b)] is less than that seen in the perpendicular K_u sample, but they show an in-plane asymmetry in the domain structure. This asymmetry in domain structure is not seen in thinner comparably prepared samples, similar to the results for the perpendicular K_u sample.

We magnetized the sample in the plane of the film and repeated the MFM and SANS analyses on this remanent state

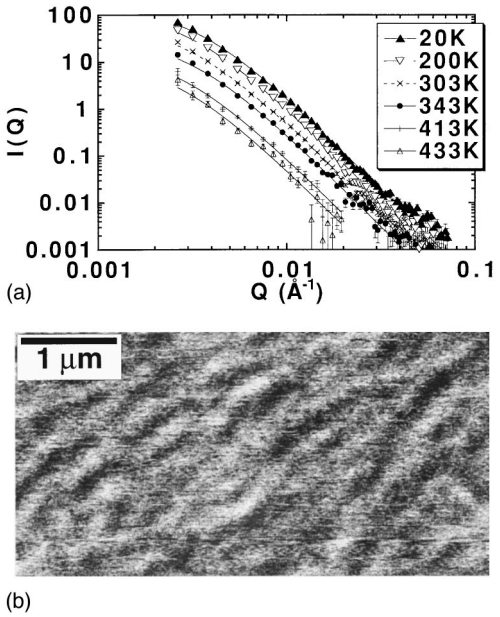

FIG. 4. (a) SANS $I(Q)$ at various temperatures and (b) MFM image measured at 300 K for thermally demagnetized state of in-plane K_u a-$TbFe_2$ (grown at 300 K and annealed at 573–623 K for 2 h). Sample total thickness 9.5 μm (seven samples stacked, each either 1 or 1.5 μm thick). $M_s=150$ emu/cc and $K_u\sim-1\times10^6$ ergs/cc at room temperature, with a strong in-plane axis (estimated at 1×10^7 ergs/cc with respect to rotation of M in plane). Fits shown in (a) are Lorentzian-squared (Lorentzian term was negligible), with a correlation length of 300 Å, independent of temperature.

(in zero field, at room temperature). The MFM image shows similar structure to that seen in the thermally demagnetized state of Fig. 4(b) but with less contrast, and the SANS intensity dropped to a level insignificantly above background. These observations suggest that MFM contrast in the remanent state is due to small variations in magnetization direction.

C. Sputtered perpendicular anisotropy sample

Figure 5(a) shows $I(Q)$ for a sputtered sample in a thermally demagnetized state and Fig. 5(b) the corresponding MFM image. This sample is 1 μm thick, grown at 493 K (220 °C) and has perpendicular $K_u=1\times10^7$ ergs/cc, comparable to the evaporated sample. Three samples were stacked together for the SANS measurements. Unlike the evaporated sample, the SANS data are isotropic in plane. However, MFM images reveal an asymmetry in domain structure similar to although somewhat weaker than that shown in Fig. 3 for the evaporated sample. It is possible that the asymmetry in domain size seen in MFM is not seen in SANS because the alignment of elongated domains is less precise than in the evaporated sample (sputtering typically preserves incident angles less than evaporation due to the randomizing influence of scattering off the sputtering gas atoms). The direction of asymmetry in domain structure seen in MFM images is again completely correlated with the incident atomic beam directions during growth (i.e., the domains are narrow along the direction parallel to the in-plane component of the incident atomic beams).

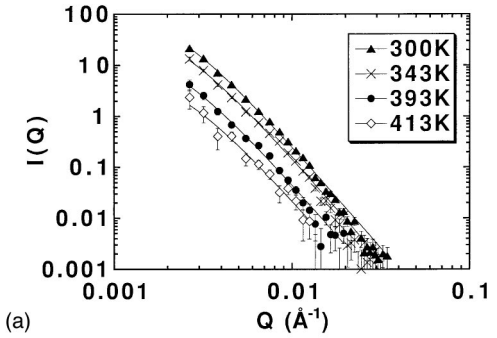

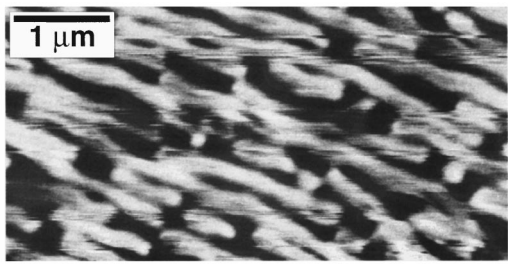

FIG. 5. (a) SANS $I(Q)$ at various temperatures and (b) MFM image measured at 300 K for thermally demagnetized state of sputtered perpendicular K_u a-$TbFe_2$ (grown at 493 K). The angle of incident atomic beams during sputter deposition is rotated approximately 90° azimuthally from that in evaporated samples; domains are elongated approximately parallel to this growth axis. Sample total thickness 3 μm (three samples stacked, each 1 μm thick). $K_u = 1\times10^7$ ergs/cc and $M_s \sim 210$ emu/cc at room temperature. Fits shown in (a) are Lorentzian squared with a correlation length of 500 Å, independent of temperature. $I(Q)$ for remanent state is barely above background; it is best fit with $1/Q^x$ with $x = 4.7$.

We magnetized the sample by applying a 15 kOe field perpendicular to the sample and remeasured it with MFM and SANS. As was seen in the evaporated perpendicular K_u sample, the MFM-imaged domains become larger and continue to show an asymmetry in size between x and y directions. The SANS intensity drops to barely above background and displays a $1/Q^x$ dependence with $x \sim 4.7$ over a narrow Q range (0.0035–0.008 Å^{-1}) before vanishing into the background noise.

IV. ANALYSIS OF SANS DATA

We have fit $I(Q)$ in Figs. 2, 4, and 5 to various functional forms, specifically the Lorentzian plus Lorentzian squared form of Eq. (2) with $\kappa = R_f^{-1}$ ($R_f^{\perp -1}$), the QLRO form of Eq. (3), and a simple $1/Q^x$ power law. In order to remove both the instrument background signal and the nonmagnetic nuclear (structural) scattering, we subtracted the data taken above T_c from all lower temperature data. This background is a negligible contribution to the total measured signal at temperatures significantly below T_c [see, for example, data in Fig. 2(a)]. We note that $I(Q)$ for all samples at all temperatures in the thermally demagnetized state has approximately the same functional form, including the data taken at the highest temperature, above T_c. This may be because the nuclear scattering has the same form as the magnetic, due to an influence of the atomic structure on the formation of magnetic structure, or it may be due to residual magnetic scattering still dominating the SANS signal at 473 K. We also note that the remanent state for all samples produces a significantly lower SANS signal than the thermally demagnetized state and (where measurable) a significantly different functional form, despite little difference in magnetization.

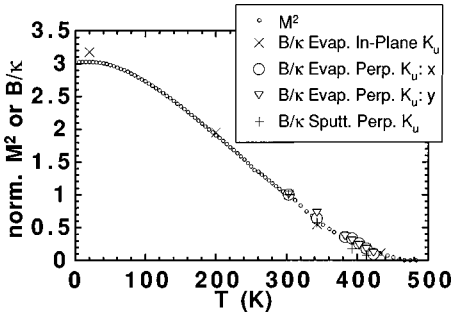

FIG. 6. Coefficient B of the Lorentzian-squared term for $I(Q)$ in Figs. 2(b)–2(d), 4(a), and 5(a), divided by κ, normalized to the value of B/κ at 300 K plotted against temperature. The small circles are $M^2(T)$ for the in-plane K_u sample shown in Fig. 4 normalized to its value at 300 K. Note the collapse of data for all samples onto a common line.

For all samples in all states, Eq. (2) provided a far better fit to the data than Eq. (3), suggesting that *none* of the samples are in the QLRO state at the measured temperatures. This is not unexpected for the samples with high perpendicular anisotropy; as discussed in the Introduction, the large uniaxial anisotropy should cause the ground state to be FM. For the in-plane anisotropy sample, it was more unexpected, since this sample was expected to be in the $m=2$, $d=3$ QLRO state. However, the discovery of a significant *in-plane* easy axis suggests that this sample also is in a FM state due to a coherent anisotropy axis.

Fitting the data to Eq. (2), we have found that for all temperatures measured (all $T<T_c$), for all samples in all states, the Lorentzian-squared term dominates and R_f ($R_f^{\perp}$) ≈ 300 Å (500–700 Å for the perpendicular anisotropy samples) and is independent of temperature (within 10–20 %). These fits are shown in Figs. 2, 4, and 5. Attempts to fit any of the data with $R_f = 50$–100 Å, the length scale found from previous results[8] on rapidly sputtered material, results in significant deviations towards a lower slope below $Q = 0.01$–0.02, which is not supported by the data. Particularly in the remanent state data of Fig. 2(d), where the magnitude of magnetic scattering at finite Q is quite small, the possibility of significant RMA-induced wandering of magnetization on a 50–100 Å length scale is remote.

In Fig. 6 we plot the coefficient B of the Lorentzian-squared term of Eq. (2) used to fit the data in Figs. 2–5, divided by κ, normalized to its value at 300 K, versus temperature. We also show $M^2(T)$ for the in-plane anisotropy sample normalized to its value at 300 K; $M(T)$ was measured by first applying a large field in plane at room temperature to magnetically saturate the sample, then measuring in 200 Oe on heating or cooling. The collapse of all the data to a single form is strong confirmation that the SANS signal is reflecting the overall bulk magnetization (squared) of the samples ($B\alpha|M|^2\kappa$). We note that κ is approximately constant with temperature, changing by less than 20% over the

entire temperature range shown, hence the temperature dependence seen in Fig. 6 is dominated entirely by the temperature dependence of B and M^2.

As discussed in the Introduction, the interpretation of a Lorentzian-squared term can be either as randomly interpenetrating magnetic domains [Debye-Bueche (DB) model], or as a wandering of magnetization due to the random anisotropy within a ferromagnetic domain induced by a coherent anisotropy axis (whether perpendicular or in-plane axis) (RMA model). Either interpretation results in $B\alpha|M|^2\kappa$ consistent with Fig. 6. The domain walls themselves will also contribute a SANS signal. Since the spins in domain walls do not rotate as an exponential correlation function, this contribution should not lead to a Lorentzian-squared term. To the best of our knowledge, such a contribution has not been calculated but may be indistinguishable from a Lorentzian squared and would also be expected to be proportional to $M^2\kappa$ if κ^{-1} is identified as the wall width (narrower walls would lead to a larger signal at a given value of Q). To distinguish between these models, we consider both the magnitude of the coherence length and the absolute magnitude of scattering, specifically the magnitude of the Lorentzian-squared coefficient B.

In the DB model, the exponential decay of the spin correlation $e^{-\kappa r}$ is due to interpenetrating domains with meandering domain walls. The DB model crosses over to a Porod $1/Q^4$ dependence for Q large compared to κ ($1/Q$ small compared to domain size). Upon examination of this expression, it is clear that the length κ^{-1} must be of order the domain size. In the thermally demagnetized state, the SANS data give $\kappa^{-1}\approx 300-500$ Å, of order 10 times $\sqrt{A/K_u}$. This length is therefore qualitatively consistent with the fastest possible wandering of magnetization in these high uniaxial anisotropy materials. The MFM images of the various samples show domains whose size qualitatively scales with κ^{-1}, although of order 5 times larger. In the remanent state for the two samples with a measurable SANS signal, SANS data indicate an approximate $1/Q^4$ dependence, suggesting that the coherence length is beyond the measured Q range ($\kappa^{-1}>1100$ Å, assuming that a 5% deviation from $1/Q^4$ would be observable at the lowest measured Q values). The MFM images are consistent with a much larger domain size in this state.

The coefficient B can be identified with the density of domain walls in the DB model; $B=(\Delta\rho)^2 S \ \alpha \ M^2 S$, where S is the density of domain walls (cm^2/cm^3) and is equal to $2\pi\kappa$. In our data, the magnitude of the coefficient B at 300 K is strongly correlated with the inverse of the domain widths seen in the MFM images and hence with the density of domain walls. Specifically, the narrower the domains, the greater the magnitude of SANS signal and hence of the coefficient B. The difference in domain-wall areal density seen in MFM then explains the difference in SANS intensity in the x and y directions and in the two different magnetic states seen for the perpendicular K_u samples. In the thermally demagnetized states, where the value of the correlation length is measurable at 300–500 Å, the absolute magnitude of scattering is consistent with the value of the correlation length and the magnetization [$B=8\pi\kappa(0.27\times 10^{-12}M/\mu_B)^2$ to within a factor of 5]. In the remanent state for the evaporated perpendicular K_u sample, the coefficient B is 10–100 times less than in the demagnetized state (x and y directions, respectively), suggesting a correlation length of 5000 Å-5 μm, outside our measured Q range, consistent with the $1/Q^4$ dependence seen in Fig. 2(d). This increased correlation length is also consistent with the large domains seen in MFM images. Similarly, the large drop in scattering amplitude for the sputtered perpendicular anisotropy sample and the evaporated in-plane anisotropy sample in the remanent state compared to the thermally demagnetized state implies a large increase in correlation length.

We note that in the large-Q Porod limit, calculations and observations on several types of samples have shown that a finite width of domain walls causes a negative curvature in SANS (or small-angle x-ray scattering) I versus Q, i.e., fits of $I(Q)$ to $1/Q^x$ give $x>4$.[45] Domain-wall widths in amorphous $TbFe_2$ are of order 100 Å, an appreciable fraction of the correlation length, hence this negative curvature is to be expected. Indeed, values of x larger than 4 (4.7–4.8) are seen in the remanent state data for both samples where the signal is significantly above background, and negative curvature deviations from pure Lorentzian-squared behavior is seen in data on both perpendicular anisotropy samples at large Q ($1/Q^x$ with $x\approx 4.6-4.8$ fits data for $Q>0.01$ Å^{-1}). For the in-plane anisotropy sample at large $Q(>0.01$ Å$^{-1})$, we see a pure $1/Q^4$ dependence of intensity. It is possible that the smaller value of κ^{-1} for this sample means that we are not yet far enough into the Porod limit to see $x>4$. Alternatively, the likely difference in spin direction *within* the domain walls in the two types of samples (perpendicular versus in-plane anisotropy) would affect the scattering and hence the magnitude of negative curvature.

If we instead interpret the SANS signal as arising directly from the finite range ordered spins in the domain walls themselves, then the correlation of the magnitude of the SANS signal with domain-wall areal density is again straightforward to explain. The deviation of spins from alignment is not an exponential function, and therefore will not lead to a Lorentzian-squared term in SANS; however, the difference could be small. The correlation length would then be related to the thickness of the wall itself, rather than its degree of meander as in the DB model. The length observed in the thermally demagnetized states is of the order of magnitude of observed domain-wall widths (a factor of 3–5 times longer). However, this model is inconsistent with the remanent state observations. In the remanent state, the measured correlation length is increased outside the range observable (pure $1/Q^4$ dependence), while the structure and width of the domain walls is unlikely to have changed at all.

The alternative interpretation of the Lorentzian-squared term is the RMA model; i.e., a wandering of the magnetization *within* each domain, with a length scale of 300–500 Å $=R_f$ or $R_f^{\perp}$. However, in this case it is difficult to understand the correlation of the coefficient B with inverse MFM-observed domain size, and particularly the near vanishing of the SANS signal in the remanent state. It is also difficult to explain R_f (or $R_f^{\perp}$) $=300$ Å at low temperature in a material for which $D/J_{ex}\sim 0.3-0.7$, unless the orientational correlation length $R_a=300$. [More precisely, as seen in Eq. (4) and the discussion following, there are two possible values for R_a for each value of R_f, the second one is, however, less than 1.5 Å, the interatomic distance.] While $R_a=300$ Å is in

principal possible, it seems implausibly long in an amorphous material. Viewing this alternatively as a ferromagnetic with a wandering axis, as appropriate for high uniaxial anisotropy samples, the expected correlation length $R_f^{\perp} = (A/K_u)^{1/2} \approx 50$ Å.[20] Again the only way to increase this theoretical length to the observed value is to increase the orientational correlation length R_a to what would appear to be an unphysical value of 500 Å in plane.

Instead of the Lorentzian plus Lorentzian-squared form, if one fits the data to a power-law $1/Q^x$ dependence, the present data has $x \sim 3.3-3.7$ for the thermally demagnetized state of all samples fit over the entire Q range measured, and $x \sim 4.7$ for the remanent state of both perpendicular anisotropy samples at room temperature. The data of Ref. 8 have $x \sim 2.4$.

One interesting and unexpected result of this study is that thick (>1 μm) amorphous $TbFe_2$ samples show a significant (factor of 10) in-plane asymmetry in magnetic domain size, correlated with the direction of the incident atomic beams and presumably related to growth-induced kinetic roughening effects. This effect was seen in both sputtered and *e*-beam coevaporated films. For thick (>1 μm) samples which have been annealed to eliminate the strong perpendicular magnetic anisotropy, in addition to an in-plane asymmetry in domain size we found a strong in-plane magnetic anisotropy axis approximately along the original incident atomic beam directions. The magnitude of this in-plane anisotropy has not been measured, but an estimate based on $M(H)$ loops in different directions is greater than 1×10^7 ergs/cc. This in-plane axis is at most weakly present in the as-deposited high perpendicular anisotropy samples. Further experiments are needed to explain how this in-plane axis develops from the original perpendicular anisotropy axis. A final note is that it is not clear why the SANS signal for the in-plane anisotropy sample is isotropic, where MFM images show anisotropic domain structure and in-plane $M(H)$ hysteresis loops indicate a large in-plane anisotropy axis. The imperfect alignment of the domain walls may lead to the isotropic SANS signal as it did for the sputtered perpendicular anisotropy sample. Alternatively, it may be related to the near alignment of elongated domains with magnetization direction, unlike for the perpendicular anisotropy samples where domains are perpendicular to the anisotropy axis. The dominant scattering due to magnetic moments is for Q perpendicular to the anisotropy axis, but is at $Q=0$ and hence unobservable.

In summary, small-angle neutron scattering and magnetic-force microscopy have been used to characterize the magnetic correlation length and the domain structure of amorphous $TbFe_2$, prepared under a variety of different conditions and in different magnetic states. Significant small-angle scattering was seen, with a temperature-dependent magnitude which correlated strongly with both the magnetic moment of the sample and with the size and shape of the domains seen in the magnetic-force microscope. SANS data are dominated by a Lorentzian-squared term for all samples in all magnetic states. The ferromagnetic correlation length found from fitting the SANS $I(Q)$ to a functional form is long (300–500 Å in the thermally demagnetized state; 10–100 times longer in the remanent state). This long length is consistent with theoretical predictions of a ferromagnetic ground state in exchange-dominated random anisotropy magnets such as amorphous $TbFe_2$ in the presence of coherent anisotropy. Both the correlation length and the absolute magnitude of SANS are strongly correlated with observed domain sizes from MFM images. We suggest that the Lorentzian-squared term may be best understood as resulting from ferromagnetic domains with meandering domain walls, similar to the Debye-Bueche model developed for particles.

ACKNOWLEDGMENTS

We would like to thank Mike Fitzsimmons and Susan Watson for their assistance with the LQD measurements; Ron Fisch for his patience and assistance in understanding RMA models; Eugene Chudnovsky, Bruce van Dover, and Michael Coey for many valuable conversations; and Karen Kavanagh, Robert Opila, and Julia Phillips for their invaluable help in characterizing these samples. We thank Takao Suzuki for support and use of the MFM/AFM at Toyota Technological Institute. Our special thanks go to the late Mike Gyorgy for his encouragement and insight in all areas of magnetism. We thank the DOE (DE-FG03-95ER45529) and the UC Campus-Laboratory Collaboration for support and gratefully acknowledge use of magnetometers at CMRR and CIMS at UCSD. This work benefitted from the use of the low-Q diffractometer, LQD, at the Manuel Lujan, Jr., Neutron Scattering Center, Los Alamos National Laboratory, funded by the U.S. Department of Energy under Contract No. W-7405-ENG-36 with the University of California.

[1] N. Heiman, A. Onton, D. F. Kyser, K. Lee, and C. R. Guarnieri, in *Magnetism and Magnetic Materials*, edited by C. D. Graham *et al.*, AIP Conf. Proc. No. 24 (AIP, New York, 1975), p. 573; R. J. Gambino, J. Ziegler, and J. J. Cuomo, Appl. Phys. Lett. **24**, 99 (1974).

[2] F. Hellman and E. M. Gyorgy, Phys. Rev. Lett. **68**, 1391 (1992); F. Hellman, R. B. van Dover, S. Nakahara, and E. M. Gyorgy, Phys. Rev. B **39**, 10 591 (1989), and references therein.

[3] R. B. van Dover, M. Hong, E. M. Gyorgy, J. F. Dillon, Jr., and S. D. Albiston, J. Appl. Phys. **57**, 3897 (1985).

[4] P. Hansen, C. Clausen, G. Much, M. Rosenkranz, and K. Witter, J. Appl. Phys. **66**, 756 (1989); D. Mergel, H. Heitmann, and P. Hansen, Phys. Rev. B **47**, 882 (1993).

[5] V. G. Harris, K. D. Aylesworth, B. N. Das, W. T. Elam, and N. C. Koon, Phys. Rev. Lett. **69**, 1939 (1992); IEEE Trans. Magn. **20**, 2958 (1992).

[6] S. N. Cheng and M. H. Kryder, J. Appl. Phys. **69**, 7202 (1991), and references therein.

[7] P. Hansen and H. Heitmann, IEEE Trans. Magn. **MAG-25**, 4390 (1989).

[8] J. J. Rhyne, S. J. Pickart, and H. A. Alperin, Phys. Rev. Lett. **29**, 1582 (1972); S. J. Pickart, J. J. Rhyne, and H. A. Alperin, *ibid.* **33**, 424 (1974); J. J. Rhyne, IEEE Trans. Magn. **MAG-21**, 1990 (1985).

[9] J. J. Rhyne, J. H. Schelleng, and N. C. Koon, Phys. Rev. B **10**, 4672 (1974).

[10] D. P. Belanger and A. P. Young, J. Magn. Magn. Mater. **100**, 272 (1991); K. Binder and A. P. Young, Rev. Mod. Phys. **58**, 801 (1986).

[11] *Magnetic Glasses*, edited by K. Moorjani and J. M. D. Coey (Elsevier, Amsterdam, 1984).

[12] R. Harris, M. Plischke, and M. J. Zuckermann, Phys. Rev. Lett. **31**, 160 (1973).

[13] Yadin Y. Goldschmidt, in *Recent Progress in Random Magnets*, edited by D. H. Ryan (World Scientific, Singapore, 1992), p. 151.

[14] D. J. Sellmyer and M. J. O'Shea, in *Recent Progress in Random Magnets* (Ref. 13), p. 71.

[15] Eugene M. Chudnovsky, *The Magnetism of Amorphous Metals and Alloys*, edited by J. A. Fernandez-Baca and Wai-Yim Ching (World Scientific, Singapore, 1995), Chap. 3, p. 143.

[16] Y. Imry and S.-K. Ma, Phys. Rev. Lett. **35**, 1399 (1975).

[17] R. A. Pelcovits, E. Pytte, and J. Rudnick, Phys. Rev. Lett. **40**, 476 (1978); R. A. Pelcovits, Phys. Rev. B **19**, 465 (1979).

[18] C. Jayaprakash and S. Kirkpatrick, Phys. Rev. B **21**, 4072 (1980).

[19] Y. Goldschmidt and A. Aharony, Phys. Rev. B **32**, 264 (1985).

[20] E. M. Chudnovsky and R. A. Serota, IEEE Trans. Magn. **20**, 1400 (1984); J. Phys. C **16**, 4181 (1983); E. M. Chudnovsky, W. M. Saslow, and R. A. Serota, Phys. Rev. B **33**, 251 (1986).

[21] C. M. Hurd, Contemp. Phys. **23**, 469 (1982).

[22] J. P. Rebouillat, A. Lienard, J. M. D. Coey, R. Arrese-Boggiano, and J. Chappert, Physica B & C **86-88B**, 773 (1977); J. W. M. Biesterbos, M. Brouha, and A. G. Dirks, *ibid.* **86-88B**, 770 (1977).

[23] R. Fisch, Phys. Rev. B **41**, 11 705 (1990); **42**, 540 (1990).

[24] R. Fisch and A. B. Harris, Phys. Rev. B **41**, 11 305 (1990).

[25] R. Fisch, Phys. Rev. B **58**, 5684 (1998).

[26] Ronald Fisch, Phys. Rev. B **51**, 11 507 (1995); Phys. Rev. Lett. **66**, 2041 (1991).

[27] R. Fisch, Phys. Rev. B **57**, 269 (1998).

[28] The ratio D/J_{ex} (or A/K_r) is complicated in a material with two magnetic ions, one (Tb) with strong anisotropy and the other (Fe) giving the strong exchange which produces a T_c well above room temperature. From mean-field analyses (Refs. 4, 46, 47), the Fe-Fe exchange is largest, the Tb-Fe exchange is approximately 1/3 of this, and Tb-Tb exchange is extremely small. The most appropriate J_{ex} is the Fe-Tb coupling constant, $\sim 1.0-1.5 \times 10^{-15}$ ergs. Then the effective value for $A \sim 0.7-1.0 \times 10^{-6}$ ergs/cm [$A = 4J_{ex}JS/\sqrt{2}d$ where $J=6$ for Tb, $S=1$ for Fe, and d refers to the Tb-Fe distance $\sim 2.5 \times 10^{-8}$ cm. The factors of 4 and $\sqrt{2}$ are numerical factors chosen by comparison to an fcc close-packed structure ($4/a$ is the usual formula where a = fcc lattice constant)]. Values for D for Dy (Tb should be comparable) in a-Dy-Ni alloys range from $3-5\ \mathrm{K} = 4-7 \times 10^{-16}$ ergs. For $D = 4-7 \times 10^{-16}$ ergs, $K_r = DN_{Tb}J^2 = 2.6-4.5 \times 10^8$ ergs/cm^3 at $T=0$ K ($N_{Tb} = 1.8 \times 10^{22}$ cm^{-3}, based on 8.3 g/cm^3 and 33 at. % Tb concentration). For a-$TbFe_2$, the observed macroscopic anisotropy K_u is as large as 1×10^7 ergs/cm^3 at room temperature and approximately three times larger at low temperatures (see, e.g., Ref. 9). K_r is thus somewhat more than a factor of 10 larger than K_u, a reasonable upper limit given the amorphous structure, where the alignment of axes is unlikely to be larger than a few %. For $D = 4-7 \times 10^{-16}$ ergs, and $J_{ex} = 1-1.5 \times 10^{-15}$ ergs, $D/J_{ex} = 0.3-0.7$ and $H_r/H_{ex} = (K_r/A)^* R_a^2 \sim 0.1-0.4$ for $R_a = 2.5$ Å. If the orientational correlation length R_a is longer, the effective value of D/J_{ex} is increased by $(R_a/a)^2$, a factor which could be large. $R_f = 50$ Å at low temperature from Ref. 8 gives $R_a \sim 2.3$ Å $\sim$ interatomic spacing, assuming $A \sim 0.7-1 \times 10^{-6}$ ergs/cm and $K_r = DN_{Tb}J^2 \sim 4 \times 10^8$ ergs/cm^3. The number of neighbors should also affect the relevant D/J_{ex} ratio; however, the number of Fe neighbors for Tb in a-$TbFe_2$ is similar to the number of magnetic neighbors in other RMA materials studied. A factor of 3 makes little difference to any of the discussion in this paper; due to the strong Tb-Fe exchange coupling, these alloys are in the moderately weak anisotropy limit unless R_a is much longer than the interatomic spacing.

[29] F. Hellman, E. N. Abarra, A. L. Shapiro, and R. B. van Dover, Phys. Rev. B **58**, 5672 (1998).

[30] B. Boucher and P. Chieux, J. Phys.: Condens. Matter **3**, 2207 (1991), and references therein.

[31] P. Debye and A. M. Bueche, J. Appl. Phys. **20**, 518 (1949); P. Debye, R. Anderson, and H. Brumberger, *ibid.* **28**, 679 (1957).

[32] D. R. Nelson, J. Non-Cryst. Solids **61-62**, 475 (1984).

[33] E. M. Chudnovsky and J. Tejada, Europhys. Lett. **23**, 517 (1993).

[34] J. M. Ruiz, X. X. Zhang, C. Ferrater, and J. Tejada, Phys. Rev. B **52**, 10 202 (1995).

[35] F. Hellman, Appl. Phys. Lett. **64**, 1947 (1994).

[36] For the *e*-beam-evaporated samples, see E. N. Abarra, Ph.D. thesis, University of California at San Diego, 1996.

[37] Working in Chudnovsky's notation, using the numbers from Ref. 28 $H_c/H_s = K_u A^3/K_r^4 R_a^6 = K_u R_f^2/A = 1$ for $K_u = 3.0-4.0 \times 10^6$ ergs/cm^3 at $T=0$ K, assuming $R_f = 50$ Å from Rhyne's measurements. Using the measured value of R_f leads to less uncertainty than the separate values of A, K_r, and R_a.

[38] G. S. Cargill and S. Kirkpatrick, in *Structure and Excitations of Amorphous Solids*, edited by G. Lucovsky, AIP Conf. Proc. No. 31 (AIP, New York, 1976), p. 339.

[39] For the sputtered samples, see Refs. 2, 3; also F. Hellman, S. Nakahara, R. P. Frankenthal, R. B. van Dover, D. J. Siconolfi, and E. M. Gyorgy, J. Appl. Phys. **65**, 2847 (1989).

[40] J-W. Lee, H-P. D. Shieh, M. H. Kryder, and D. E. Laughlin, J. Appl. Phys. **63**, 3624 (1988); F. Hellman and K. Kavanagh (unpublished); also see, for example, A. G. Dirks and H. J. Leamy, Thin Solid Films **47**, 219 (1977); N. G. Nakhodkin and A. I. Shaldervan, *ibid.* **10**, 109 (1972); J. A. Thornton, J. Vac. Sci. Technol. **12**, 830 (1975), and recent conferences on kinetic roughening.

[41] P. A. Seeger, R. P. Hjelm, and M. Nutter, Mol. Cryst. Liq. Cryst. **180A**, 101 (1990).

[42] P. A. Seeger and R. P. Hjelm, J. Appl. Crystallogr. **24**, 467 (1991).

[43] R. P. Hjelm, J. Appl. Crystallogr. **21**, 618 (1988).

[44] See, for example, F. Family, Physica A **168**, 561 (1990); C. Tang, S. Alexander, and R. Bruinsma, Phys. Rev. Lett. **64**, 772 (1990).

[45] P. W. Schmidt *et al.*, J. Chem. Phys. **94**, 1474 (1991); W. Ruland, J. Appl. Crystallogr. **4**, 70 (1971); J. Coberstein, B. Morra, and R. Stein, *ibid.* **13**, 34 (1980).

[46] A. Gangulee and R. C. Taylor, J. Appl. Phys. **49**, 1762 (1978); A. Gangulee and R. J. Kobliska *ibid.* **49**, 4896 (1978).

[47] M. Mansuripur and M. F. Ruane, IEEE Trans. Magn. **MAG-22**, 33 (1986).